

*VERTICAL CHEMISTRY OF THE THREE DYNAMICALLY  
DIFFERENT REGIONS OF THE BLACK SEA*

*KARADENİZ'İN ÜÇ FARKLI DİNAMİK BÖLGESİNİN DÜŞEY KİMYASI*

ÖZDEN BAŞTÜRK, SÜLEYMAN TUĞRUL, İLKAY SALİHOĞLU

Middle East Technical University, Institute of Marine Sciences (IMS-METU), Erdemli  
İcel, Turkey.

**Key Words:** Black Sea, chemical properties, upwelling, downwelling, rim current

**Abstract**

In the upper layer of the Black Sea, the vertical distributions of nutrients and dissolved oxygen display very characteristic features at specific density surfaces. Moreover, data from a survey in September 1991 indicate that the positions and magnitudes of these properties show small regional differences from the core of the cyclonic gyres towards the anticyclonic eddies established in the coastal regions. The nutricline always appeared at shallower depths but at greater density surfaces within the cyclonic gyres. The molar ratios of N:P reached peak values of as much as 100 at the upper boundary of the nitracline due to a consistent shift between the onsets of the nitracline and the phosphocline. The sub-surface phosphate minimum is a permanent feature of the cyclonic regions; however, it almost disappears in the meandering rim current, yielding lower concentrations at the depth of the deep phosphate maximum coinciding with the onset of the sulphidic waters.

**Introduction**

Recent investigations indicate dramatic changes have occurred in the principal biological and chemical properties of the Black Sea during last two decades due to various interacting factors. For instance, chemical pollution of the riverine inflows has resulted in intense eutrophication, especially in the northwestern and western shelf waters (Mee, 1992; Bodeanu, 1992) though the fresh water inputs have been reduced by about 50% in the last two decades (Tolmazin, 1985; Fashchuck and Ayzatullin, 1986). During the same period, the entire Black Sea ecosystem has been invaded by opportunistic organisms (Vinogradov *et al.*, 1989; Shuskina and Musaeva, 1990; Smayda, 1990). In addition to ecological changes in the productive surface layer, the upper boundary of the oxic/anoxic transition layer has risen toward the surface (Murray *et al.*, 1989; Tuğrul *et al.*, 1992).

However, since 60's the onset of sulphidic water over the deep basin has remained almost constant at about the same density surface (Tuğrul *et al.*, 1992; Saydam *et al.*, 1993; Baştürk *et al.*, 1994; Buesseler *et al.*, 1994) though its actual depth varies markedly with region (Bezberodov, 1990).

It is well known that the vertical chemistry of the Black Sea below the euphotic zone is principally determined by the variabilities in meso-scale circulations and the consequent hydrographic features. Accordingly, density dependent chemical profiles in the upper layer of the Black Sea have been found to be more informative in examining long-term, basinwide data (Murray *et al.*, 1989; Codispoti *et al.*, 1991; Tuğrul *et al.*, 1992; Oğuz *et al.*, 1991; Saydam *et al.*, 1993). However, the positions and magnitudes of the characteristic chemical features, such as the boundaries of the nutricline, oxycline, suboxic zone and the maxima and minima of phosphate and nitrate profiles, may be expected to exhibit noticeable and consistent spatial and temporal differences when density dependent profiles from hydrodynamically different regions are compared. To consider this, we here examine the basin-wide chemical data collected during the September-1991 cruise, together with the Knorr-1988 and Atlantis-1969 data sets.

### **Materials and Methods**

Water samples were collected by rosette casts at pre-determined density surfaces. Nutrients were measured on board the R/V Bilim (IMS-Turkey) using a two-channel Technicon Autoanalyzer. Dissolved oxygen was determined by a semi-automatic Winkler titration modified slightly for low oxygen concentrations. Sampling flasks for the dissolved oxygen and hydrogen sulphide were flushed with argon gas and kept closed until the sub-sampling. Solutions containing standardized iodine solutions and sample water were titrated against the standardized thiosulfate solution as given in APHA-AWWA-WPCP Standard Methods (Greenberg *et al.*, 1985). A Sea-Bird Model-9 CTD probe provided physical data throughout HydroBlack-91 multi-ship cruise. Chemical and physical data of the R/V Knorr (USA) and R/V Atlantis (USA) cruises were taken from the reports of Friederich *et al.*, (1990) and Brewer (1971), respectively.

### **Results and Discussions**

Spatial variabilities in the principal hydrochemical properties of the Black Sea upper layer extending down to the anoxic layer can be deduced from the comparison of composite profiles. Old and recent data sets were therefore grouped in three sub-regions, by taking into account the position of each station in terms of the dynamic height anomalies in cm at the 100 dbar level relative to the 900 dbar level (Fig. 1). The coordinates of sampling locations are listed in Table 1.

**Regional Variations in the Physical Properties:** Fig.1 shows that, in September 1991, there existed two cyclonic gyres in the interiors of the eastern and western basins of the Black Sea; these gyres were separated from a series of anticyclonic eddies in coastal zones by the meandering rim current which was found to be as wide as 75 km and to possess an

Figure 1. Dynamic height anomalies in cm at 100 Dbar level  
relative to 900 Dbar level in September 1991

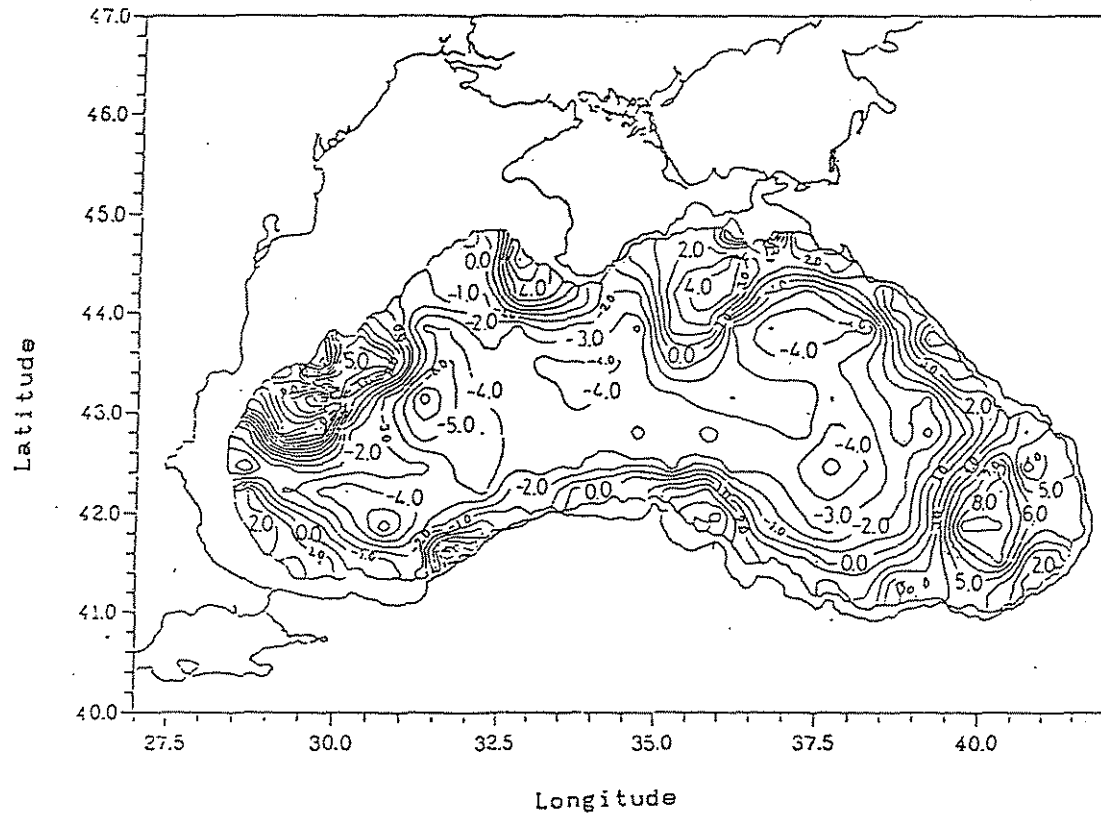


Table 1. The station names and coordinates used in the text for three different regions of the Black Sea and for three different cruises.

CYCLONIC GYRE			ANTICYCLONIC GYRE			RIM CURRENT		
Sta.	Lat.	Long.	Sta.	Lat.	Long.	Sta.	Lat.	Long
			R/V BILIM - 1991					
N30N45	43° 30'N	31° 45'E	L50Y15	41° 50'E	40° 15'E	L30W45	41° 30'N	38° 45'E
M50T45	42° 50'N	36° 45'E	L15Y15	41° 15'E	40° 15'E	L30W15	41° 30'N	38° 15'E
M10V15	42° 10'N	37° 15'E	L30X45	41° 30'E	39° 45'E	L15W15	41° 15'N	38° 15'E
M50P45	42° 50'N	32° 45'E	L30Y50	41° 30'E	40° 50'E	L32M13	41° 32'N	30° 13'E
M50N45	42° 50'N	31° 45'E	L30Y15	41° 30'E	40° 15'E	L30V45	41° 30'N	37° 45'E
M30N45	42° 30'N	31° 45'E	M10X45	42° 10'E	39° 45'E	L31V22	41° 31'N	37° 22'E
M30P15	42° 30'N	32° 15'E	L30X15	41° 30'E	39° 15'E	M19R45	42° 19'N	37° 45'E
N10R45	43° 10'N	34° 45'E	L50X15	41° 50'E	39° 15'E	L45T45	41° 45'N	36° 45'E
			R/V KNORR - 1988					
KNORR-1	41° 52'N	31° 19'E	KNORR-2	41° 31'N	40° 45'E	KNORR-3	41° 35'N	32° 00'E
			R/V ATLANTIS - 1969					
1444	43° 49'N	31° 41'N	1468	42° 00'N	40° 00'E	1431	42° 10'N	33° 00'E
1442	44° 45'N	31° 58'E	1469	41° 24'N	40° 41'E	1438	41° 58'N	35° 40'E
1446	42° 13'N	31° 29'E	1470	42° 02'N	41° 18'E	1440	42° 12'N	34° 21'E
1445	43° 08'N	31° 27'E	1477	41° 34'N	39° 03'E	1447	41° 22'N	30° 59'E

average speed of 20 cm/s in the surface layer (Oğuz *et al.*, 1993). The quasi-permanent anticyclonic Batumi eddy was located at the southeastern corner of the Black Sea where the boundary current moves offshore and the geostrophic surface currents exceed 30 cm/s (Oğuz *et al.*, 1991, 1993; Sur *et al.*, 1994).

Composite depth profiles of temperature (T), salinity (S) and potential density ( $\sigma_\theta$ ) in Fig.2 for the cyclonic, anticyclonic and meandering rim current regions permit us to collate spatial changes in the vertical distributions of these properties over the basin. In the cyclonic gyres, the T, S and  $\sigma_\theta$  profiles of individual stations were similar below 35-40 m, whereas the profiles from the anticyclonic eddies possessed remarkable local differences down to at least 200 m depth. However, below 70-80 meters, the profiles from the meandering rim current resemble those from the cyclonic gyres. These profiles clearly demonstrate that, below the seasonal pycnocline, there exists a nearly isohaline and relatively cool, isothermal water mass of some 10 meters thickness within the anticyclonic eddies; it becomes very thin in the cyclonic gyres (Fig. 2). The thickness of this layer also determines the thickness of the Cold Intermediate Layer (CIL) defined by the upper and lower 8 °C isothermals.

Various suggestions have appeared on the formation of the CIL over the Black Sea basin (Filippov, 1965; Ovchinnikov and Popov, 1986) and its subsequent advection (Oğuz *et al.*, 1993). The Brunt-Visl frequency was reported to be minimum at the depth of the  $\sigma_\theta=14.7$  isopycnal surface and reached maximum value below the 14.8 surface which corresponds not only to approximate base of the temperature minimum in the CIL, but also to the upper boundary of the permanent pycnocline (Buesseler *et al.*, 1994; Murray *et al.*, 1991). Thus, one suggests that the surface layer may be homogenized down to the 14.6-14.7 isopycnal surfaces by convective mixing processes during the winter period.

**Regional Variations in the Chemical Properties:** The vertical distributions of nutrients ( $\text{o-P}_4$  and  $\text{N}_3+\text{N}_2$  (TNOx)) with respect to the water density are illustrated in Fig.3 for the cyclonic, anticyclonic and the rim current systems of the Black Sea. The composite profiles from the hydrodynamically different regions exhibit characteristically similar vertical features in the intermediate water column extending from the base of the euphotic zone to the upper anoxic layer as recently emphasized by Tuğrul *et al.*(1992), Murray *et al.*(in press) and Saydam *et al.*(1993). However, detailed examination of these density-dependent composite profiles has led to the identification of certain spatial differences both in the positions and concentrations of the principal chemical features that consistently appear at specific density surfaces as discussed below.

**Distributions of Nutrient Elements:** The  $\text{o-P}_4$  and TNOx concentrations of the productive surface waters of the Black Sea were both less than 0.1-0.2  $\mu\text{M}$  due to the assimilation by autotrophic species (Fig. 3). The nutrient deficient layer extends down to the  $\sigma_\theta=14.5$ -14.6 surfaces in the cyclonic gyres, but only to the  $\sigma_\theta=14.2$ -14.3 surfaces in the other two systems (Fig. 2). Accordingly, the onset of the nutricline coinciding with the permanent pycnocline was located at different density surfaces. It appeared at greater density surfaces but at relatively shallower depths (25-30m) in the cyclonic gyres than

Figure 2. Composite depth dependent variations of temperature, salinity and sigma-t within dynamically different regions of the Black Sea. (A): cyclonic, (B): anti-cyclonic and (C): rim current for September-1991 period

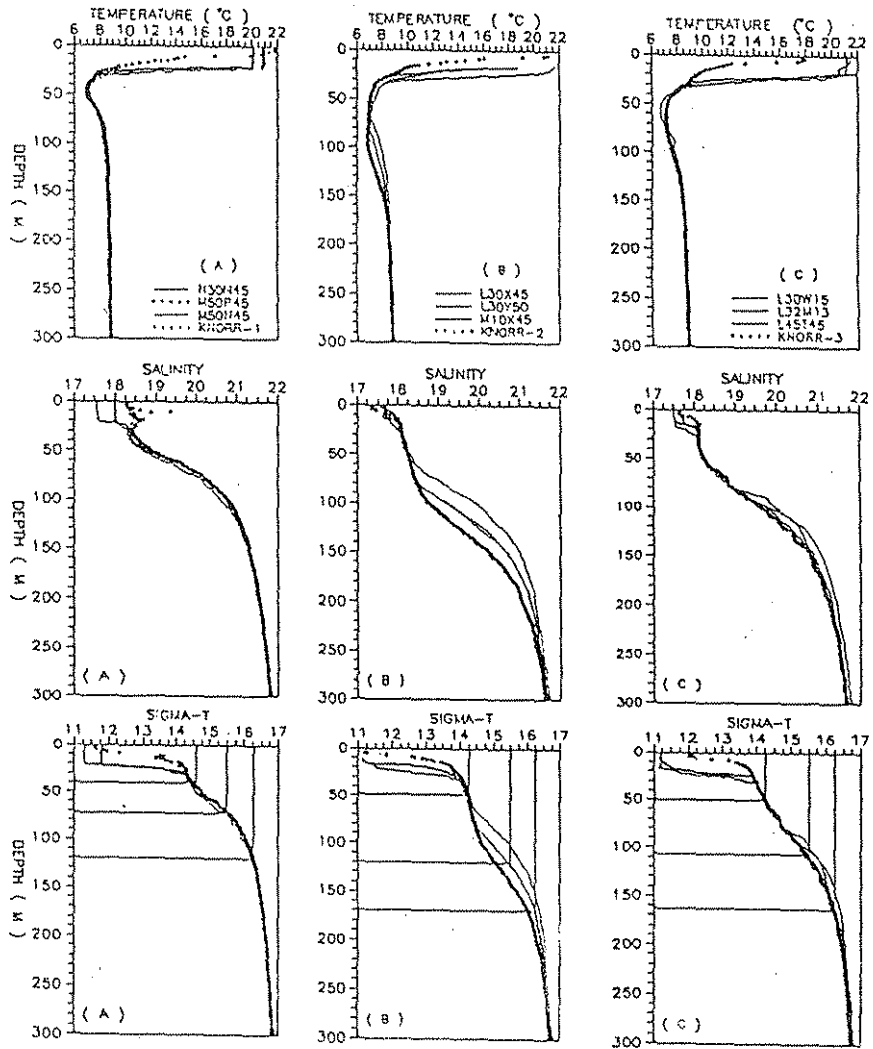
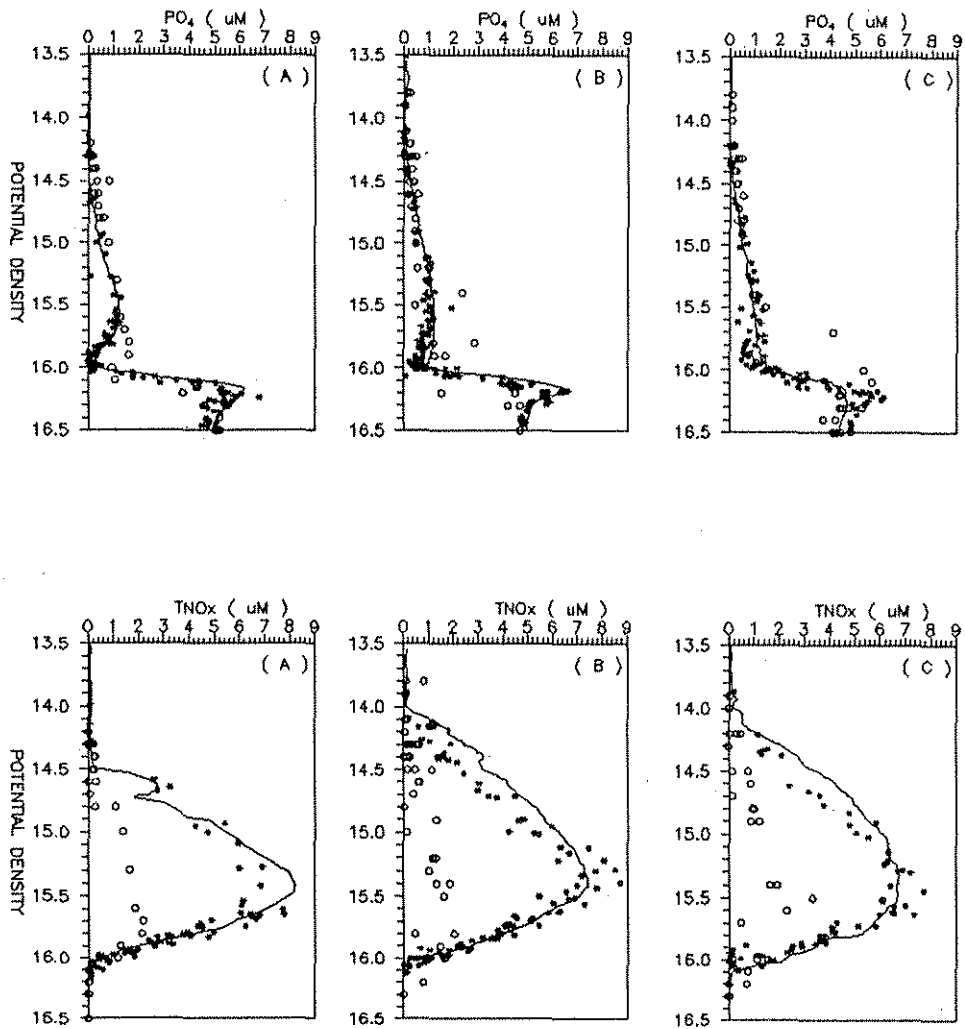


Figure 3. Composite potential density dependent variations of  $\sigma\text{-PO}_4$  and  $\text{TNO}_x$  species within dynamically different regions of the Black Sea for (A): cyclonic, (B): anti-cyclonic and (C): rim current. (R/V Bilim (\*), R/V Knorr (--) and R/V Atlantis (o))



those in the anticyclonic eddies and rim current where it was as deep as 40-60 meters (Fig. 2). Such a distinctive spatial difference in the onset of the nutricline is the result of the differences in the formation and position of the CIL in these regions. For instance, in the anticyclonic eddies,  $1 \mu\text{M}$   $\text{o-P}_4$  concentration was reached at about  $\sigma_\theta=15.20$  surface whereas it first appeared at the depth of  $\sigma_\theta=15.4-15.5$  surfaces within the cyclonic gyres (Fig. 3).

The sub-basin composite  $\text{o-P}_4$  profiles (Fig. 3) exhibit two characteristic maxima and a sub-surface minimum within the suboxic zone; the upper maximum is relatively broad, reaching to peak values between the 15.5-15.7 isopycnal surfaces in the cyclonic and anticyclonic regions. This feature almost disappears in the rim current frontal zone. Below the upper, relatively sharp maxima of the cyclonic regions, the profiles display a steep decreasing trend down to the  $\sigma_\theta=15.85-15.90$  surfaces. In this zone, the concentrations were as low as  $0.05-0.10 \mu\text{M}$  in the core of the cyclonic gyres, but increased towards the peripheries as a result of intense vertical and horizontal mixings. Thus, the sub-surface phosphate minimum, yielding a mean of  $0.21 \mu\text{M}$  for the cyclonic gyres, weakens significantly in the anticyclonic regions ( $0.97 \mu\text{M}$ ) and becomes almost undetectable in the rim current zone, where phosphate concentrations were in the range of  $1.0-1.2 \mu\text{M}$  between  $\sigma_\theta=15.85-15.95$  surfaces (Table 2 and Fig. 3). This minimum has been suggested to arise from the scavenging of dissolved phosphate ions by metal (primarily Fe and Mn) oxides as they sink through the oxic waters into the reductive, anoxic zone (Shaffer, 1986; Spencer and Brewer, 1971) or alternatively by dissolved Mn(II) (Tebo, 1991) and Mn(III) ions (Luther, 1991) in vertically stable systems. In fact, the contact of the sub-oxic zone with the reducing sediments of the coastal margins (Kempe *et al.*, 1991) introduces reduced Fe and Mn species to the oxic layer where the oxidized metal compounds may be expected to export more phosphate from the oxic into the anoxic layer than in the offshore waters. This suggestion is supported by the larger concentrations of particulate Mn-oxide observed within the suboxic zone of the coastal margins (Tebo, 1991). However, the strong boundary current near the Anatolian coast enhances the vertical and horizontal mixing and inhibits the development of the phosphate minimum within the suboxic zone (Codispoti *et al.*, 1991). However, it is as yet unclear what major bio-mediated chemical processes contribute to the formation of the characteristic phosphate minima within the suboxic zone of cyclonic gyres.

The phosphate concentration increases steeply within the base of the suboxic zone irrespective of location (Fig. 3); the concentrations, as low as  $0.1-1.2 \mu\text{M}$  in the sub-surface minimum zone, reach to peak values of  $5-7 \mu\text{M}$  at the  $\sigma_\theta=16.20-16.25$  surfaces and then decrease slowly in the upper anoxic waters. The maxima consistently appear at the sulphidic water boundary throughout the deep basin, probably resulting from dissolution of the phosphate-associated metal oxides in the anoxic waters (Shaffer, 1986; Codispoti *et al.*, 1991). The disappearance of the sub-surface phosphate minimum within the rim current zone, together with the lower values of the deep phosphate maxima at the sulphidic boundary, strongly suggests that a significant quantity of phosphate is exported from the upper anoxic water into the suboxic zone of the coastal waters and then were



probably advected by the meandering rim current towards the interior of the basin as was suggested by Lewis and Landing (1991).

Composite TNOx vs density profiles (Fig. 3) demonstrate that in the anticyclonic eddies and the rim current, the nitracline onset was located at the  $\sigma_\theta=14.2-14.3$  surfaces whereas it was at the  $\sigma_\theta=14.4-14.5$  surfaces within the cyclonic gyres, corresponding nearly to the base of the euphotic zone. The prominent nitrate maximum which is a permanent property of the basin were consistently established between the  $\sigma_\theta=15.35-15.45$  surfaces throughout the basin; the averages of the peak values were 8.00 and 7.84  $\mu\text{M}$  for the cyclonic and anticyclonic regions, and 7.80  $\mu\text{M}$  for the rim current (Fig. 3 and Table 2). It should be noted that the nitrate maxima were always located at the base of the oxycline where DO concentration dropped to suboxic values of 20-30  $\mu\text{M}$  and the phosphate concentrations being as high as 1.06-1.14  $\mu\text{M}$  (Table 2). The TNOx concentrations declined to 0.1-0.2  $\mu\text{M}$  within the suboxic/anoxic transition zone and eventually to undetectable levels in the upper anoxic water.

A detailed examination of the nutrient profiles reveals a noticeable shift between the onsets of TNOx and  $\text{P}_4$  gradients. The phosphocline commenced at deeper density surfaces, a shift of about 0.1-0.2  $\sigma_\theta$  units, compared to the nitracline ( $\sigma_\theta=14.2-14.5$ ) for all three regions. It should also be noted that the onsets of the reactive silicate gradient (Fig. 4) coincide with the nitracline onsets for three regions. Such a consistent shift between the onsets of TNOx and o- $\text{P}_4$  gradients always occurs within the upper CIL where the average salinity was 18.49, 18.19 and 18.21 ppt for the cyclonic, anticyclonic and rim current regions, respectively.

The depth-integrated totals of TNOx, o- $\text{P}_4$  and DO and the corresponding molar TNOx: $\text{P}_4$  ratios between the oxycline and the suboxic zone of the three regions are given in Table 3. The oxygen and nutrient contents of the oxycline were much larger in the anticyclonic than in the cyclonic region; it originates principally from large differences between the oxycline were much larger in the anticyclonic than in the cyclonic region; it originates principally from large differences between the oxycline (thus nutricline) thicknesses of these dynamically different regions where the peak values of chemical concentrations were comparable. The nutricline thickness increases from 30-40 m in the cyclonic to about 70-80 in the anticyclonic regions (Fig. 2). In the suboxic zone, the depth-integrated DO and o- $\text{P}_4$  values were still larger in the anticyclonic regions, but the TNOx estimates appeared to be comparable (Table 3). The TNOx: $\text{P}_4$  ratios estimated from the regressions in the oxycline ranged merely between 7.0 and 8.2, which were much less than the conventional Redfield Ratio of 16 estimated for the oceans. The ratio decreased to levels of 4.5-6.6. within the suboxic zone of the Black Sea due to the suppression of TNOx removal by intense denitrification over the  $\text{P}_4$  removal to the anoxic waters.

The TNOx gradient within the oxycline appeared to range from 0.207  $\mu\text{M}/\text{m}$  for cyclonic gyres to 0.123  $\mu\text{M}/\text{m}$  for anticyclonic eddies and 0.133  $\mu\text{M}/\text{m}$  for rim current system, due to a two-fold regional difference in the nutricline thickness. Below the TNOx maxima, the nitrate depletion rate changed insignificantly with region, from an estimated 0.216  $\mu\text{M}/\text{m}$  in the anticyclonic eddies to 0.227 and 0.240  $\mu\text{M}/\text{m}$  for the cyclonic gyres and the rim current regions. This suggests that the TNOx losses from the suboxic zone are comparable

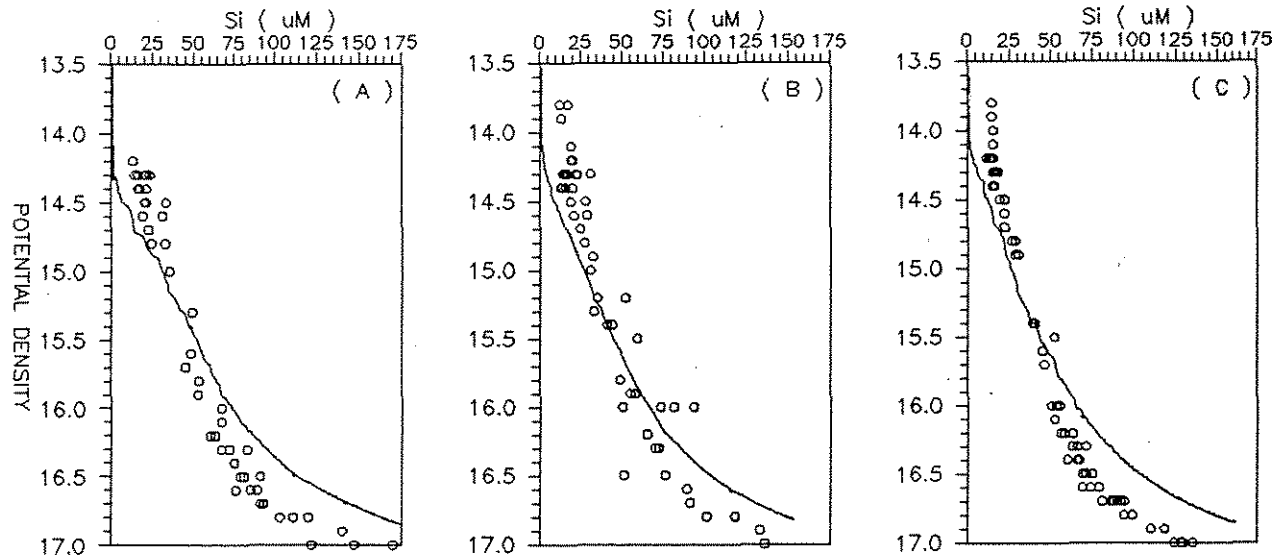
Table 2. Averages of saturated dissolved oxygen (SDO), dissolved oxygen (DO), o-PO<sub>4</sub> and TNOx concentrations and corresponding averaged depths of the density surfaces (DDS) within dynamically different regions of the Black Sea.

POTENTIAL DENSITY SURFACE INTERVALS									
$\sigma_{\theta} = 14.20 - 14.30$			$\sigma_{\theta} = 15.35 - 15.45$			$\sigma_{\theta} = 15.95 - 16.00$			
A	B	C	A	B	C	A	B	C	
SDO	331.7	340.6	336.8	327.0	327.1	327.2	321.8	321.8	321.9
DO	323.4	279.8	261.6	21.7	30.2	21.7	3.7	3.3	4.9
o-PO <sub>4</sub>	0.02	0.02	0.01	1.07	1.06	1.14	0.21	0.97	1.20
TNOx	0.14	1.23	1.16	8.00	7.84	7.80	1.29	0.93	0.97
DDS	28-32	46-62	40-47	67-69	121-124	90-96	95-99	154-157	119-124
(A): Cyclonic gyre, (B): Anticyclonic gyre, (C): Rim current									

Table 3. Depth integrated totals of dissolved oxygen (DO), o-PO<sub>4</sub> and TNOx concentrations within  $\sigma_{\theta} = 14.30-15.40$  and  $\sigma_{\theta} = 15.41-15.95$  isopycnal surfaces for different dynamic regions of the Black Sea (All are in units of  $\times 10^{-3}$  moles.m<sup>-2</sup>)

$\sigma_{\theta} = 14.30 - 15.40$				$\sigma_{\theta} = 15.41 - 15.95$		
	A	B	C	A	B	C
DO	3371.7	7494.1	4837.0	298.8	602.3	391.2
PO <sub>4</sub>	12.4	23.9	21.3	19.9	27.3	28.3
TNOx	86.9	196.1	151.3	130.8	143.7	128.3
N/P	7.0	8.2	7.1	6.6	5.3	4.5
(A): Cyclonic gyre, (B): Anticyclonic gyre, (C): Rim current						

Figure 4. Composite potential density dependent variations of silicate within dynamically different regions of the Black Sea for (A): cyclonic, (B): anti-cyclonic and (C): rim current. (R/V Bilim (\*), R/V Knorr (--)) and R/V Atlantis (o))



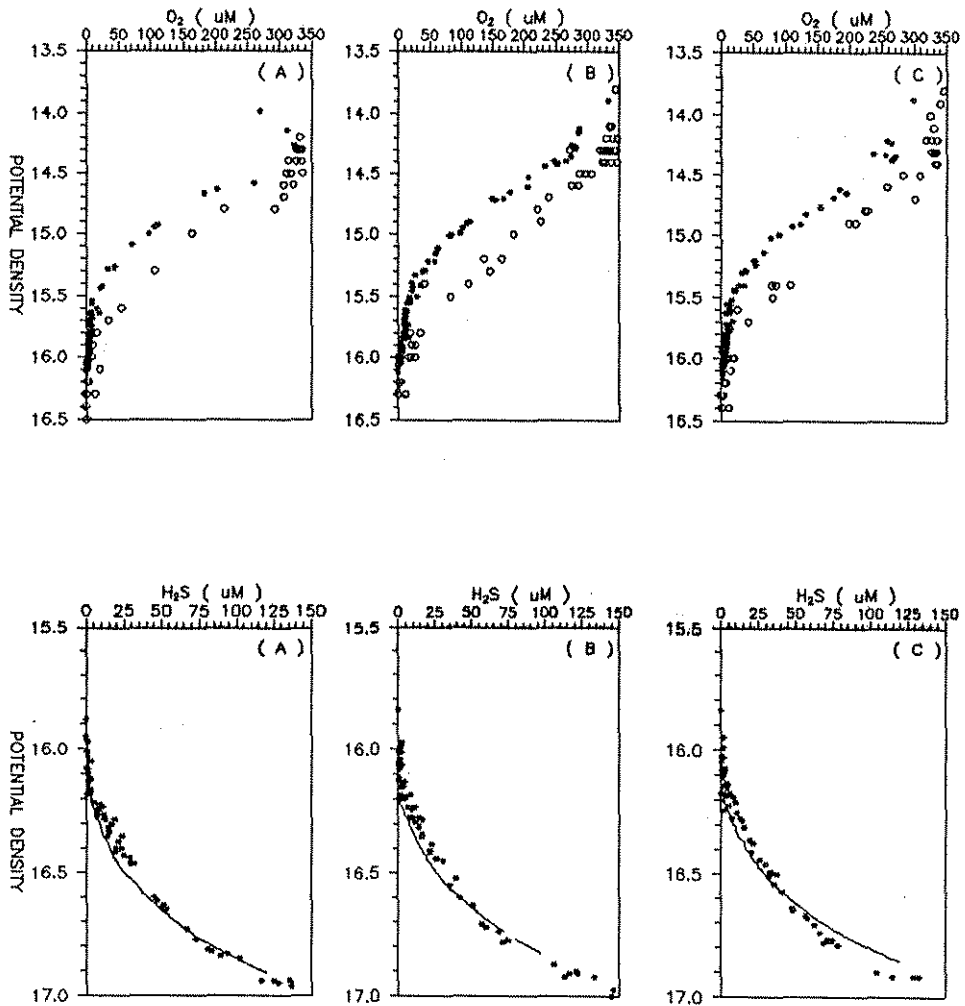
throughout the basin, whereas the phosphate gradient changes markedly with region due to the spatial variability in the redox-dependent processes. Light transmittance data measured during the Knorr-88 and Bilim-91 cruises support this suggestion because regionally varying intensities of minima were recorded within the anoxic interface, indicating the existence of a fine particle layer between 15.95-16.20 surfaces. The pronounced transmission minima in the rim current zone have most probably originated from the resuspension of sedimentary particles by vertical mixing and horizontal advection induced by the strong boundary currents attached to the coastal zone which in turn prevent the formation of the sub-surface phosphate minimum (Kempe *et al.*, 1991).

**Dissolved Oxygen and Hydrogen Sulphide:** Sub-basinwide dissolved oxygen profiles (Fig. 5) indicate that the DO concentrations, ranging between 250-350  $\mu\text{M}$  in the productive surface layer, decreased steeply to suboxic values of 20-30  $\mu\text{M}$  at the 15.4-15.5 density surfaces where the nitrate maximum was established (Table 2). However, the upper boundary of the oxycline was observed at greater density surfaces ( $\sigma_\theta=14.4-14.5$ ) within the cyclonic gyres whereas it was established just below  $\sigma_\theta=14.2-14.3$  within the anticyclonic eddies and the rim current region. These surfaces are naturally expected to define the nutricline onset. Because of the spatial shift in the onset of the oxycline, the DO gradients estimated from the composite profiles in Fig. 5 change markedly with region, from 7.94  $\mu\text{M}/\text{m}$  within the cyclonic to 3.57  $\mu\text{M}/\text{m}$  for the anticyclonic regions and to 4.60  $\mu\text{M}/\text{m}$  for the rim current. Because of insufficient ventilation, the DO concentrations decline slowly from 20-30  $\mu\text{M}$  at the base of the main oxycline ( $\sigma_\theta=15.4-15.5$ ) to  $<5$   $\mu\text{M}$  at the 15.9-16.0 isopycnal surfaces, with the lower gradient values in a range between 0.84-0.93  $\mu\text{M}/\text{m}$  for the anticyclonic and the rim current regions and of 0.61  $\mu\text{M}/\text{m}$  for the cyclonic region. This oxygen-poor water mass defines the boundaries of the suboxic zone extending from the main oxycline at  $\sigma_\theta=15.4-15.5$  surfaces to the sulphidic water onset at  $\sigma_\theta=16.15-16.20$  surface throughout the deep basin.

The changes in the molar ratios of AOU:N:P estimated from the averages given for the  $\sigma_\theta=14.2-14.3$  and  $\sigma_\theta=15.35-15.40$  density surfaces (Table 2) are 283:7.5:1 and 227:6.4:1 for the cyclonic and anticyclonic regions, respectively, and 195:5.9:1 for the rim current. These ratios differ significantly from the conventional estimates of 175:16:1 for the deep ocean (Takahashi *et al.*, 1985). In other words, besides oxygen losses due to the oxidation of organic matter, losses from the thin oxycline to the suboxic zone by diffusive processes are much larger in the cyclonic gyres than in the anticyclonic eddies. However, in the rim current frontal zone, such losses are compensated by oxygen inputs from the upper, oxic layer. Comparison of ratios also reveals that the nitrate losses from the nutricline exceed the phosphate removal even though the chemical composition of biogenic particles deviates to some extent from the Redfield ratio as observed in the Sea of Marmara fed by the surface inflow from the western Black Sea (Polat, 1995).

Although the ratios of the AOU:TNOx between 14.2 and 15.4 density surfaces are nearly the same, 38:1, 36:1 and 33:1 for cyclonic, anticyclonic and rim current regions, they differ significantly between the 15.4 and 16.0 surfaces where the lowest value (1.9:1) was observed in cyclonic gyres compared to those in anticyclonic (3.2:1) and rim current

Figure 5. Composite potential density dependent variations of dissolved oxygen and hydrogen sulfide within (A): cyclonic, (B): anti-cyclonic and (C): rim current regions of the Black Sea. (R/V Bilim (\*) and R/V Knorr (--))



regions (3.1:1), implying that the nitrogen removal by the denitrification processes exceeds that of oxygen. In other words, the main oxidant for the oxidation of reduced species, such as Fe(II), Mn(II), H<sub>2</sub>S and even NH<sub>4</sub> diffusing from the anoxic zone, as was suggested by Murray *et al.*, (in press), is the TNO<sub>x</sub> rather than very low levels of dissolved oxygen.

Composite profiles of H<sub>2</sub>S derived from the titrimetric measurements are illustrated in Fig. 5, together with the high-precision data of the Knorr-88 cruise obtained by continuous profiling system. Comparison of profiles strongly suggests that concentrations from the HydroBlack-91 cruise were consistently overestimated by at least 5 µM within the low-lying anoxic waters due to inadequate estimation of the system blank in the anoxic transition layer. According to HydroBlack-91 data, the sulphidic water with a concentration of 3-5 µM H<sub>2</sub>S first appears at the 16.10-16.15 isopycnal surfaces whereas it was recorded consistently at nearly σ<sub>θ</sub>16.2 surface during the Knorr-88 cruise throughout the deep basin. Between the 16.10-16.15 and 16.30 isopycnal surfaces, the mean gradients of the composite H<sub>2</sub>S profiles were estimated as 0.73 µM/m for the cyclonic, 0.58 µM/m for the anticyclonic and 0.51 µM/m for the rim current frontal zones (including the uncertainty arising from analytical artifacts), whereas the Knorr-88 data indicate much less regional differences in the H<sub>2</sub>S gradients in the upper anoxic waters.

## Özet

Karadeniz üst tabaka sularında besin tuzları ve çözünmüş oksijen konsantrasyonlarının düşey dağılımları belirli yoğunluk (σ<sub>θ</sub>) yüzeylelerinde özgün dağılım özellikleri göstermektedir. Eylül-1991 saha çalışmalarının sonuçlarından, bu özelliklerin büyüklük ve düşey konumlarının, siklonik bölge merkezlerinden kıyasal bölgelerde gözlenen anti-siklonik bölgelere gidildikçe bazı bölgesel farklılıklar gösterdiği; yine besin tuzlarının, siklonik döngülerde anti-siklonik döngülere oranla daima daha sığ derinliklerde fakat daha yüksek σ<sub>θ</sub> değerlerinde artmaya başladığı anlaşılmaktadır. Molar N/P oranları, nitraklin (nitracline) tabakası üst kesimlerinde tepe değerlerine ulaşmakta olup bu oran bazen 100'u aşabilmektedir. Söz konusu tepe değerleri, nitraklin ve fosfoklin tabakalarının başlangıç yoğunluk yüzeyleleri arasındaki 0.1 σ<sub>θ</sub> birimlik kaymadan kaynaklanmaktadır. Yüzeyle-altı tabakada gözlenen PO<sub>4</sub>-minimum tabakasının siklonik bölgelerde belirgin bir şekilde gözlenmesine rağmen, bu tabaka oluşumu anti-siklon bölgelerinde azalmakta, kıyasal akıntı (Rim current) bölgesinde, anoksik tabaka üst sınırının (σ<sub>θ</sub>=16.15-16.20) gözlenen PO<sub>4</sub>-maksimumundaki azalmaya paralel olarak, tamamen yok olmaktadır.

## Acknowledgments

This work was supported by the Turkish Scientific and Technical Council (TÜBİTAK) and the NATO-Science for Stability Program. The authors wish to thank the crew of R/V Bilim and the technicians in the IMS for their valuable contributions.

## References

- Baştürk, Ö., Saydam, C., Salihoğlu, İ., Ereemeev, L.V., Konovalov, S.K., Stoyanov, A., Dimitrov, A., Cociasu, A., Dorogan, L., and Altabet, M. (1994) Vertical variations in the principle chemical properties of the Black Sea in the autumn of 1991, *Marine Chemistry* 45: 149-165.
- Bezberodov, A.A. and Ereemeeva, V.I. (1990) The boundary of hydrogen sulfide in the Black Sea in 20's and 80's, *Morsk. Gidrofiz. Zh.* 5: 62-64 (in Russian).
- Bodeanu, N. (1992) Algal blooms and development of the main planktonic species at the Romanian Black Sea littoral in conditions of intensification of the eutrophication process, in R.A. Wollenweider, R. Marchetti and R.V. Viviani (eds.), *Marine Coastal Eutrophication*, Elsevier Publ., Amsterdam, pp.891-906.
- Brewer, P.G. (1971) Hydrographic and chemical data from the Black Sea, Woods Hole Oceanogr. Inst. Technical Report, Reference No:71-65.
- Buesseler, K.O., Livingston, H.D., Ivanov, L., and Romanov, A. (1994) Stability of the oxic-anoxic interface in the Black Sea, *Deep Sea Res.* 41(2): 283-296.
- Carpenter, E.J. and Capone, D.G. (1983) *Nitrogen in the Marine Environment*, Academic Press, London.
- Codispoti, L.A., Friederich, G.E., Murray, J.W., and Sakamoto, C.M. (1991) Chemical variability in the Black Sea: Implications of continuous vertical profiles that penetrated the oxic/anoxic interface, *Deep-Sea Res.* 38(2A): 691-710.
- Fashchuk, D.YA. and Ayzatullin, T.A. (1986) A possible transformation of the anaerobic zone of the Black Sea, *Oceanology* 26(2): 171-178.
- Filipov, D.M. (1965) The cold intermediate layer in the Black Sea, *Oceanology* 5: 47-52.
- Friederich, G.E., Codispoti, L.A., and Sakamoto, C.M. (1990) *Bottle and pumpcast data from the Black Sea expedition*, Monterey Aquarium Research Institute Tech. Rep. 90-3, 224p.
- Greenberg, A.E., Trussell, R.R. and Clesceri, L.S. (1985) Standard methods for the examination of water and wastewaters, APHA-AWWA-WPCF Publ.
- Kempe, S., Diercks, A.R., Liebezeit, G., and Prange, A. (1991) Geochemical and structural aspects of the pycnocline in the Black Sea (R/V Knorr 134-8 Leg 1, 1988), in E. Izdar and J.W. Murray (eds.), *Black Sea Oceanography*, NATO-ASI Series C, vol.351, Kluwer Acad. Publ., Netherlands, pp.89-110.
- Lewis, B.L. and Landing, W.M. (1991) The biogeochemistry of manganese and iron in the Black Sea, *Deep-Sea Res.* 38(20): S773-S803.
- Luther, G.W. (1991) Sulfur and iodine speciation in the water column of the Black Sea, in E. Izdar and J.W. Murray (eds.), *Black Sea Oceanography*, NATO-ASI Series C, vol.351, Kluwer Acad. Publ., Netherlands, pp.187-204.
- Mee, L.D. (1992) The Black Sea in crisis: The need for concerted international action, *Ambio* 21: 278-286.
- Murray, J.M., Jannasch, H.W., Honjo, S., Anderson, R.F., Reeburgh, W.S., Top, Z., Friederich, G.E., Codispoti, L.A., and Izdar, E. (1989) Unexpected changes in the oxic/anoxic interface in the Black Sea, *Nature* 338: 411-413.
- Murray, J.M., Top, Z., and Ozsoy, E. (1991) Hydrographic properties and ventilation of the Black Sea, *Deep-Sea Res.* 38(2): S663-S690.

- Murray, J.M., Codispoti, L.A. and Friederich, G.E. (in press) Redox environments: The suboxic zone in the Black Sea, in C.P. Huang, C.R. O'Melia and J.J. Morgan (eds.) *Aquatic Chemistry*, American Chemical Society.
- Oğuz, T., Latif, M.A., Sur, H.İ., Özsoy, E., and Ünlüata, Ü. (1991) On the dynamics of the southern Black Sea, in E. İzdar and J.W. Murray (eds.), *Black Sea Oceanography*, NATO-ASI Series C, vol.351, Kluwer Acad. Publ., Netherlands, pp:43-63.
- Oğuz, T., Latun, V.S., Latif, M.A., Vladimir, V.V., Sur, H.İ., Markov, A.A., Özsoy, E., Kotovhchikov, B.B., Ereemeev, V.V., and Ünlüata, Ü. (1993) Circulation in the surface and intermediate layers of the Black Sea, *Deep-Sea Res.* 40(8): 1597-1612.
- Ovchinnikov, I.M. and Popov, YU.I. (1987) Cold-intermediate layer formation in the Black Sea, *Oceanology* 27(5): 739-746.
- Polat, Ç.S. (1995) Nutrient and organic carbon budgets in the Sea of Marmara: A progressive effort on the biogeochemical cycles of carbon, nitrogen and phosphorus, Ph.D. Thesis, Institute of Marine Sciences, Erdemli, Icel, Turkey, June 1995.
- Saydam, C., Tuğrul, S., Baştürk, Ö., and Oğuz, T. (1993) Identification of the oxic/anoxic interface by isopycnal surfaces in the Black Sea, *Deep-Sea Res.* 40(7): 1405-1412.
- Shaffer, G. (1986) Phosphate pumps and shuttles in the Black Sea, *Nature* 321, 515-517.
- Shushkina, Eh.A., and Musaeva, Eh.I. (1990) Structure of planktonic community from the Black Sea epipelagical and its changes as the result of the introduction of a ctenophore species, *Oceanology* 30(2): 306-310.
- Smayda, T.J. (1990) Novel and nuisance phytoplankton blooms in the sea: Evidence for a global epidemic, in E. Granelli, B. Sundstroem, L. Elder and D.M. Anderson (eds.), Lund, Sweden, 26-30 June, 1989, pp.29-40.
- Spencer, D.W. and Brewer, P.G. (1971) Vertical advection, diffusion and redox potentials as controls on the distribution of manganese and other trace metals dissolved in waters of the Black Sea, *J. Geophysical Res.* 76: 5877-5892.
- Sur, H.İ., Özsoy, E., and Ünlüata, Ü. (1994) Boundary current instabilities, upwelling, shelf mixing and eutrophication processes in the Black Sea, *Progress in Oceanography* 33(4): 249-302.
- Takahashi, T., Broecker, W.S., and Langer, S. (1985) Redfield ratio based on chemical data from isopycnal surfaces, *J. Geophysical Res.* 90: 6907-6924.
- Tebo, B.M. (1991) Manganese (II) oxidation in the suboxic zone of the Black Sea, *Deep-Sea Res.* 38: S883-S905.
- Tolmazin, D. (1985) Changing coastal oceanography of the Black Sea. I: Northwest shelf, *Progress in Oceanography* 15: 217-276.
- Tuğrul, S., Baştürk, Ö., Saydam, C., and Yılmaz, A. (1992) Changes in the hydrochemistry of the Black Sea inferred from water density profiles, *Nature* 359: 137-139.
- Vinogradov, M.Ye., Shushkina, E.A., Musaeva, Eh.I., and Sorokin, Yu.I. (1989) The comb-jelly *Mnemiopsis leidyi* (A. Agassiz) (Ctenophora: Lobata); a newly introduced species in the Black Sea, *Oceanology* 29(2): 293-299.

Received 2.2.1996